Chemical Source Classification in Naturally Turbulent Plumes

ARTICLE *in* ANALYTICAL CHEMISTRY · DECEMBER 2007

Impact Factor: 5.64 · DOI: 10.1021/ac0710376 · Source: PubMed

3 AUTHORS, INCLUDING:

Tim C Pearce
University of Leicester
53 PUBLICATIONS **879** CITATIONS

SEE PROFILE

Chemical Source Classification in Naturally Turbulent Plumes

Tim C. Pearce,*,† Jing Gu,† and Eric Chanie‡

Centre for Bioengineering, University of Leicester, Leicester LE1 7RH, United Kingdom, and Alpha M.O.S., 10 Avenue Didier Daurat, 31400 Toulouse, France

The spatiotemporal dynamics of chemical plumes in natural environments imposes complex time-varying responses on chemical detectors, challenging the use of conventional chemical analysis instrumentation, which often relies upon precisely controlled sampling of analytes. Insects take a different approach to this problem, typically exposing their diversity of chemical receptors to the full extent of the space−time dynamics inherent to these environments. Here we adopt a similar approach, by exposing differentially tuned chemosensor arrays to analytes dispersed in naturally turbulent chemical plumes from a point source. We propose a novel sensor preprocessing metric for complex time-varying chemosensor responses, termed sensor variation, which after normalization generates a stable array response fingerprint representative of the analyte generating the response, and is invariant to changes in distance from the source and source volumes. When applied to chemosensor array response time series, the resultant fingerprints are demonstrated to reliably support chemical classification of a group of pure analytes advected from a point source. By comparing classification performance to the same analytes at equivalent concentrations in controlled sampling conditions, we show that chemical source classification can be achieved in turbulent chemical plumes with similar accuracy to controlled experimental conditions.

Animals commonly identify chemical sources from molecules dispersed within their environment. Many invertebrates, for instance, are known to use airborne chemicals to infer information about source chemical composition, concentration, and physical location.[1] The moth, in particular, routinely performs conspecific mate location across large distances using chemical cues transported within naturally turbulent plumes.[2] This is achieved through a highly specialized olfactory pathway that exploits mixed populations of specific and broadly tuned olfactory receptors.[3] The combined population response from this repertoire of receptors with mixed specific and unspecific tunings provides a fingerprint that has been shown to represent complex mixtures of analytes more efficiently than perfectly specific chemical receptors alone.[4]

The distal positions of chemical receptors outside of the aerodynamic shadow and boundary layer introduced by these animals also means that the olfactory receptor population of many invertebrates potentially has full access to the advection and mixing processes driving the chemical stimulus. These chemical plumes are extremely rich in spatiotemporal dynamics,[2,5,6] which causes the receptor population responses to vary in both space[7,8] and time.[9−11] These spatiotemporal dynamics inherent to chemical plumes have been shown to encode information about chemical composition, source quantities, and physical location[12,13] that can potentially be decoded through subsequent sensory neural processing in the animal. How invertebrates use these time-varying array signals arising from chemical plumes for navigation and chemical source identification is not well understood. Yet, the ability of insects to exploit these time-varying chemical signals raises the question of developing remote analytical instruments for identifying chemical sources and their location based upon similar sampling principles.

A bioinspired technological approach to chemical analysis is well established through the construction of arrays of chemosensors comprising diverse population responses to complex mixtures reminiscent of those found in biology.[14] Such chemosensor arrays have been successfully applied to chemical analysis of single compounds and complex mixtures and are particularly valuable when the range of compounds to be analyzed is not known in advance. Yet, these chemosensor array systems typically rely upon

* Corresponding author: (phone) +44 (0) 116 223 1307; (fax) +44 (0) 116 252 2619; (e-mail) t.c.pearce@le.ac.uk.

† University of Leicester.

‡ Alpha M.O.S.

(1) Bell, W. J.; Kipp, L. R. In *Chemical Ecology of Insects 2*; Cardé, R. T., Bell, W. J., Eds.; Chapman and Hall: New York, 1995; pp 105−152

(2) Murlis, J.; Elkinton, J. S.; Cardé, R. T. *Annu. Rev. Entomol.* **1992**, *37*, 505−532.

(3) Todd, J. L.; Baker, T. C. In *Insect Olfaction*; Hansson, B. S., Ed.; Springer: Berlin, 1999; pp 67−96.

(4) Sanchez-Montanes;, M. A.; Pearce, T. C. *BioSystems* **2002**, *67*, 229−238.

(5) Farrell, J. A.; Murlis, J.; Long, X.; Li, W.; Carde, R. T. *Environ. Fluid. Mech.* **2002**, *2*, 143−169.

(6) Justus, K. A.; Murlis, J.; Jones, C.; Carde, R. T. *Environ. Fluid. Mech.* **2002**, *2*, 115−142.

(7) Galizia, C. G.; Sachse, S.; Rappert, A.; Menzel, R. *Nat. Neurosci.* **1999**, *2*, 473−478.

(8) Meijerink, J.; Carlsson, M. A.; Hansson, B. S. *J. Comp. Neurol.* **2003**, *467*, 11−21.

(9) Brown, S. L.; Joseph, J.; Stopfer, M. *Nat. Neurosci.* **2005**, *8*, 1568−1576.

(10) Vickers, N. J.; Christensen, T. A.; Baker, T. C.; Hildebrand, J. G. *Nature* **2001**, *410*, 466−470.

(11) Lei, H.; Christensen, T. A.; Hildebrand, J. G. *J. Neurosci.* **2004**, *24*, 11108−11119.

(12) Murlis, J.; Jones, C. D. *Physiol. Entomol.* **1981**, *6*, 71−86.

(13) Murlis, J.; Willis, M. A.; Cardé, R. T. *Physiol. Entomol.* **2000**, *25*, 211−222.

(14) Pearce, T. C; Schiffman S. S., Nagle N. T.; Gardner J. W., Eds. *Handbook of Machine Olfaction: Electronic Nose Technology*; Wiley-VCH: Weinheim, 2003

10.1021/ac0710376 CCC: $37.00
Published on Web 00/00/0000

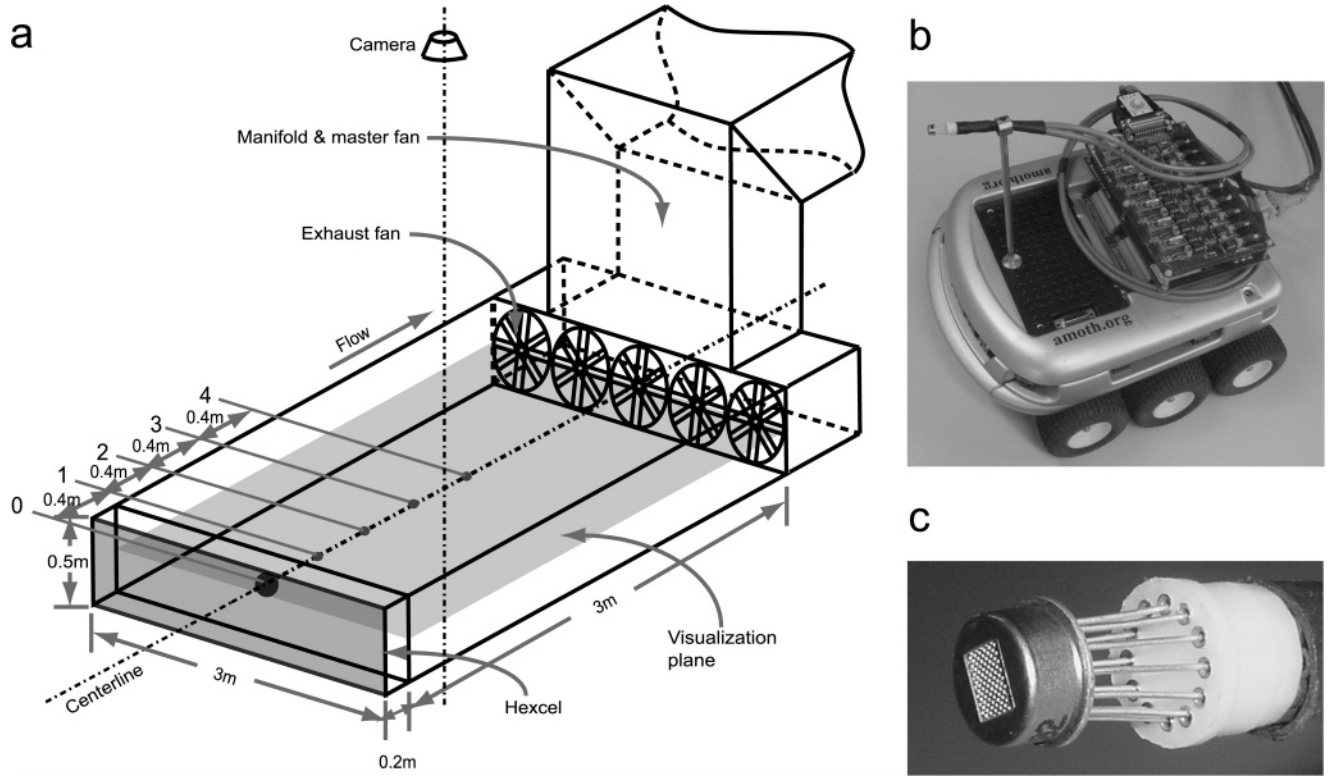

Figure 1. (a) Schematic of the wind tunnel. The wind tunnel is 3 m × 3 m × 0.5 m with manifold. The master fan generates negative pressure resulting in a controlled air flow. Five individual speed controlled fans at the end of the wind tunnel balance the air flow across its cross section. At the entrance of the wind tunnel, hexcel material of 1-cm diameter is used to remove large eddies at the inlet. The chemical source is placed at position 0 (denoted by the black circle). A six-element thin-film metal oxide chemical sensor array is placed at positions 1−4 (denoted by the small gray circles). Both source and sensor are placed at the centerline of the wind tunnel, where the gray layer indicates the plane of visualization. A CCD camera with wide-angle lens is mounted above the wind tunnel for flow visualization. Slide projectors (not shown) are used to illuminate a thin layer of flow inside the wind tunnel (gray layer). (b) Koala robot (supplied by K-team) with chemical sensor array and acquisition board. (c) The 6-element chemical sensor array package.

controlled experimental conditions (including temperature, humidity, concentration, and flow rate), very dissimilar to those found in natural chemical environments. In this case, chemosensor array signals are intentionally isolated from the natural stimulus dynamics in an attempt to optimize the reproducibility of measurements. As a result, any natural dynamics relating to the stimulus are lost during sampling and so this approach is not well suited to the problem of chemical source identification in chemical plume environments. Here we take the opposite approach, to expose chemosensor arrays to the full extent of natural plume dynamics in order to assess what information these signals contain about the source.

Various studies have focused on the problem of source localization using temporal cues obtained from chemical plumes,[15−21] but none have considered how population responses of differentially tuned chemosensor arrays may be used to identify and classify chemical sources in these environments. We can think of this as the "where" problem of chemical source localization. However, here we address the "what" problem, that is whether time-varying responses from chemical sensor arrays exposed directly to chemical plumes can be used to classify the identity of distal chemical sources rather than their position. We do this by conducting a chemical classification study in naturally turbulent plumes of different volatile compounds. In particular, we wanted to find a simple measure of time-varying chemosensor responses, suited to source classification in chemical plumes. In order to assess the robustness of our measure for chemical plume classification, we assess the sensor array response measures for different source volumes, distances from the source, flow velocities, and sampling times. By way of comparison, we tested the classification performance of an identical chemosensor array in turbulent and controlled steady-state flow conditions to demonstrate the effectiveness of these technologies for chemical plume source identification.

EXPERIMENTAL SECTION

Wind Tunnel. Experiments took place inside a wind tunnel (Figure 1a) (approximately 3 m (width) × 3 m (length) × 0.8 m (height)), constructed from transparent polyethylene sheeting. Hexcel material (aluminum honeycomb, with 1-cm diameter) at the inlet of the wind tunnel is used in order to remove the large-

(15) Balkovsky, E.; Shraiman, B. I. *Proc. Natl. Acad. Sci. U.S.A.* **2002**, *99*, 12589−12593.
(16) Ishida, H.; Nakamoto, T.; Moriizumi, T.; Kikas, T.; Janata, J. *Biol. Bull.* **2001**, *200*, 222−226.
(17) Ishida, H.; Nakayama, G.; Nakamoto, T.; Moriizumi, T. *IEEE Sens. J.* **2005**, *5*, 537−545.
(18) Ishida, H.; Nakamoto, T.; Moriizumi, T. *Sens. Actuators, B,* **1998**, *49*, 52−57.
(19) Kikas, T.; Ishida, H.; Webster, D. R.; Janata, J. *Anal. Chem.* **2001**, *73*, 3662−3668.
(20) Kikas, T.; Janata, P.; Ishida, H.; Janata, J. *Anal. Chem.* **2001**, *73*, 3669−3673.
(21) Kikas, T.; Ishida, H.; Janata, J. *Anal. Chem.* **2002**, *74*, 3605−3610.

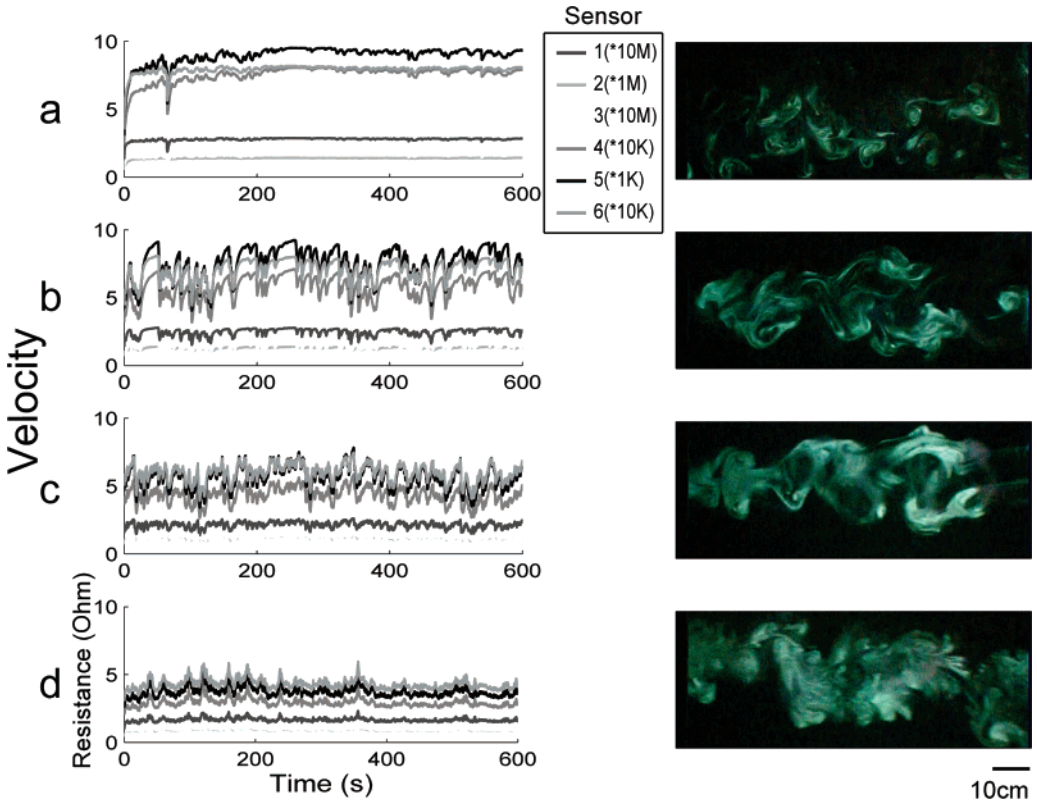

Figure 2. Chemosensor dynamics in response to an ethanol chemical plume and plume visualization inside the wind tunnel. Here the chemosensor was placed 1.5 m downwind from a 30-mL ethanol source. Measurements were taken at 10 Hz. for 10 min, at different flow velocities: (a) 0.28; (b), 0.42, (c) 0.56, and (d) 0.70 m s^{-1}. At each flow velocity, the corresponding chemical plume is visualized at the same height as the chemosensor (right column). (sensor baseline values: sensor 1, 6 MΩ; sensor 2, 0.5 MΩ; sensor 3, 1.2 MΩ; sensor 4, 17 kΩ; sensor 5, 2.0 kΩ; sensor 6, 5 kΩ).

scale eddies from the air flow. A controllable master fan (4.4 kW) is installed in a steel manifold at the outlet to produce a flow velocity in the range 0−1 m s^{-1}. Five individually controllable exhaust fans are installed between the wind tunnel and the manifold, which may be balanced to generate a uniform and symmetric flow across the wind tunnel cross section, as verified by time-averaged hot-wire anemometer measurements.

Plume Visualization. A smoke generator (Concept Smoke Systems, London, UK) was used to produce ∼1-μm-diameter oil/alcohol droplets to seed the flow from a single point of injection (nozzle diameter 2.5 cm) for the purposes of flow visualization. A camcorder (Panasonic DV 300, Matsushita Electric Industrial, Osaka, Japan) was mounted directly above the wind tunnel to capture the plume images. Four slide projectors were placed at both sides of the wind tunnel (2 at each side) with light slits focused on a plane at the height of the chemical sensor to make a thin layer of smoke plume visible. This arrangement gave rise to a small beam divergence, illuminating not more that 2-cm depth of the plume at any point in the wind tunnel. The camcorder was focused on the 1 × 1 m central field of the wind tunnel to visualize the plume.

Chemical Sensor Array. Chemical plumes were measured using an integrated thin-film metal oxide six-element chemosensor array (package size 1 cm^2, sensor spacing 500 μm, Alpha MOS SA), where sensors 1−5 are n-type metal oxide semiconductor tin oxide (SnO_2), sensors 2 and 4 are doped with catalytic metals, palladium, and platinum, respectively, while sensor 6 is a p-type metal oxide semiconductor niobium oxide (Nb_2O_5) (Figure 1c). The operating temperatures for these sensors are 400−500 °C (through a constant voltage source of 1.8 V). The heating resistors are as follows: 10 MΩ for sensors 1 and 2, 1 MΩ for sensor 3, 4, and 6, and 100 kΩ for sensor 6.

Robot Platform. A Koala robot (K-Team, Switzerland) (Figure 1b) was used as a convenient mobile platform for the chemosensor array, which allows for accurate positioning of the chemosensor within the wind tunnel. During each measurement the robot is held stationary.

Chemical Sources. Acetone (99%, Tennants), ammonia solution (∼35% NH_3 v/v, Hogg Laboratories), ethanol (99.99%, BWR), and propanol (99% purity v/v, Fisher Scientific) selected for their volatility and efficacy in producing a response in the chemosensor. Chemicals were delivered into the wind tunnel by absorbent material, which was placed at the central line of the wind tunnel, close to the inlet, at the same height as the chemosensor (marked as position 0 in Figure 1a).

Data Collection. In order to capture the sensor dynamics during exposure to naturally turbulent plumes, we recorded resistance time series generated from the six chemosensors at four different sensor positions (marked as 1−4 in Figure 1a) and for four different chemical sources. Each chemical was tested four times at each sensor position, leaving sufficient time in between tests for the sensor to recover its baseline conductance. Thus, 64 data series of sensor responses were recorded in total. Average flow velocity inside the wind tunnel was set to be 0.56 m s^{-1} and was maintained throughout all trails. For each trail, 30 mL of chemical was dispensed onto absorbent material and placed at

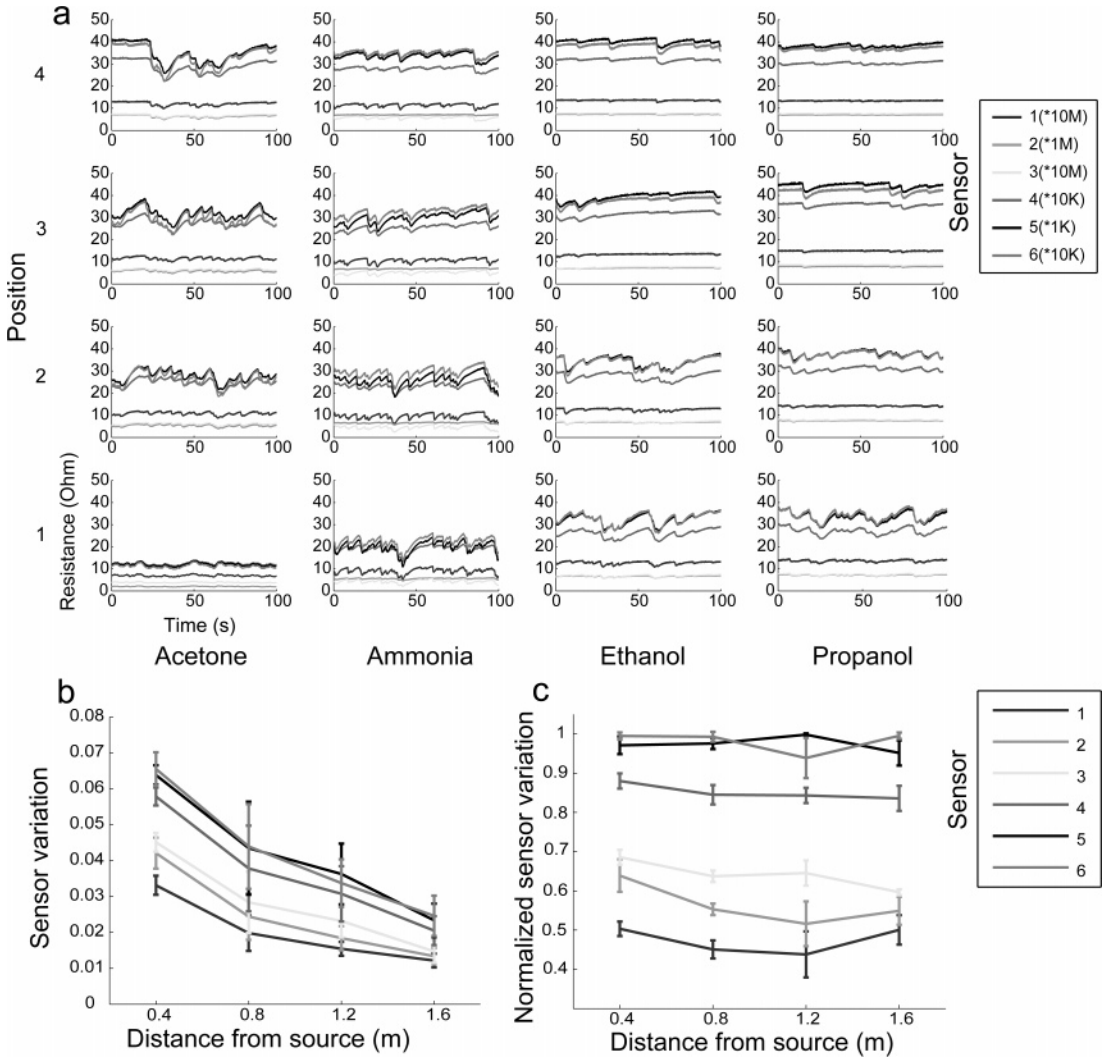

Figure 3. (a) Dynamic response of the 6-element chemosensor responding to different chemical sources at different downwind positions. Measurements were taken at 100 Hz for 10 s in total. Decreasing magnitude in sensor resistance can be seen as the chemosensor approaches the source. (b) and (c) Sensor variation and normalized sensor variation at different distances from the source. Sensor variation decreases with the distance from the source (b), while normalized sensor variation is relatively constant (c), Error bars correspond to ± standard deviation (flow velocity 0.56 m s^{-1}, position along centerline: (1) 40, (2) 80, (3) 120, and (4) 160 cm. Sensor baseline values: sensor 1, 6 MΩ; sensor 2, 0.5 MΩ; sensor 3, 1.2 MΩ; sensor 4, 17 kΩ; sensor 5, 2.0 kΩ; sensor 6, 5 kΩ).

the source location (marked as position 0 in Figure 1a). Before each new trial, the wind tunnel was left for 2−3 min for the previous odor to be cleared and the new sample to establish a concentration field. Meanwhile the chemical sensor array heaters were powered on to allow heater resistance to return to baseline. During each trail, data were logged from the chemosensor array for 100 s, sampled at a regular frequency of 100 Hz. The order of the chemicals tested and the location of the chemical sensor array were randomly selected from the set, to avoid systematic error (bias) in the data.

In a separate experiment to test the effect of different chemical source volumes, we also collected data under identical conditions at the same sensor position (marked as position 3 in Figure 1a) but for 5-, 10-, 20-, and 40-mL source volumes of all chemicals,

For comparison, we also recorded the sensor resistance responses to the same chemicals under controlled experimental conditions using an automatic headspace autosampler. The analytes were prepared in solution (by diluting with distilled water to 0.05% v/v ammonia and 0.01% v/v acetone, ethanol, and propanol) in order to produce average chemosensor array responses equivalent to those observed in the wind tunnel experiments. Liquid samples were preheated to 308.15 K and equilibrated for 600 s. Headspace from equilibrated samples was injected into an air carrier flow of 150 mL min^{-1} at a rate of 750 μL s^{-1} for acetone and 1250 μL s^{-1} for ammonia, ethanol, and propanol. Due to the high flow rate of odor delivery in the autosampler, the transient responses of the chemosensor array in this setup is largely governed by the sensor kinetics. Responses from chemosensors placed in this flow were sampled at 2 Hz for 120 s. Each compound was tested for 10 repeat trails and 20 min was left between each trail for sensor recovery.

RESULTS AND DISCUSSION

Time-Varying Chemosensor Array Responses in Turbulent Chemical Plumes. Identifying chemicals in a natural environment is a difficult task due to heterogeneity in the concentration field and filamentous nature of the chemical signal, as governed by plume dynamics.[13] In order to better understand the relation-

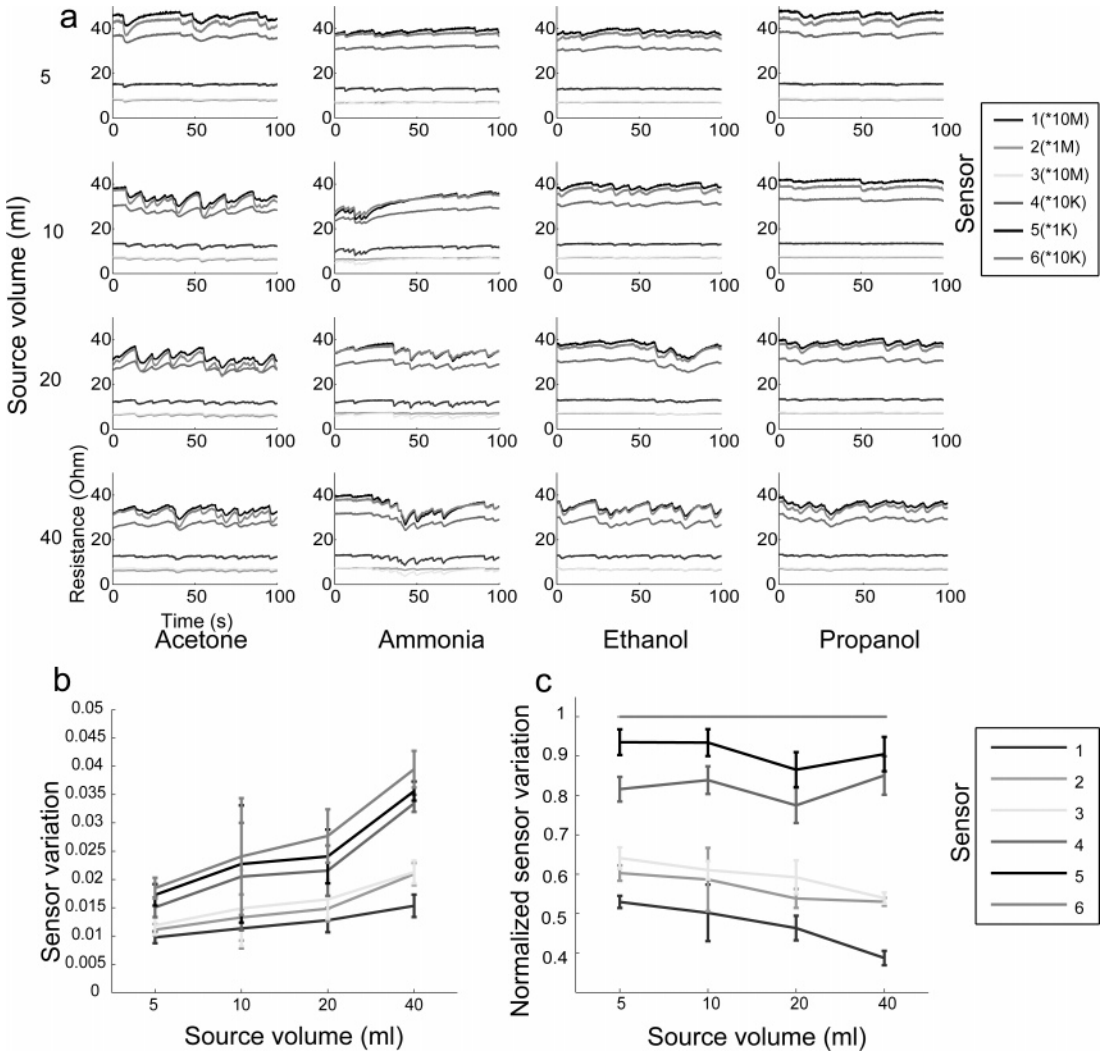

Figure 4. (a) Dynamic response of the 6-element chemosensor responding to different chemical sources at different source volumes. Measurements were taken at 100 Hz for 10 s in total. Decreasing magnitude in sensor response (resistance) can be seen as the source volumes increase. (b) and (c) Sensor variation and normalized sensor variation to different source volumes. Sensor variation increases with source volume (b), while normalized sensor variation is relatively constant (c). Error bars correspond to ± standard deviation (flow velocity 0.56 m s^{-1}, position along centerline 120 cm. Sensor baseline values: sensor 1, 6 MΩ; sensor 2, 0.5 MΩ; sensor 3, 1.2 MΩ; sensor 4, 17 kΩ; sensor 5, 2.0 kΩ; sensor 6, 5 kΩ).

ship between time-varying chemosensor array responses in chemical plumes and the plume properties, we recorded the instantaneous chemosensor array (see Experimental Section) responses within a seeded flow that was simultaneously visualized at four different flow velocities (Figure 2). In this case, the seeding compound was selected for flow visualization but also for its efficacy in producing a response in the chemosensor array. In this way, it was possible to directly compare the chemosensor response with the qualitative properties of the chemical plume.

At low flow velocities, vizualization uncovers a high degree of patchiness in the chemical flow field (Figure 2a, right), characterized by tight filaments of relatively high concentration, interspersed by little or no chemical signal. In this case, local concentration peaks are larger and received more regularly at the plume centerline, whereas here the chemosensor was slightly off-center, showing a strongly transient response when contacting one of these filaments (Figure 2a, left).

For higher flow velocities (Figure 2b,c right), greater turbulence leads to more mixing of the flow, thus spreading the chemical signal in space. In this case, the sensor signal contains rich temporal dynamics that correspond to the filaments of the passing chemical plume (Figure 2b,c left). For still greater velocity, increasing levels of turbulence mix the flow locally, resulting in less defined structure, which ultimately remove the filaments completely (Figure 2d right). This also results in less temporal structure in the chemosensor response, which is seen to be more uniform over time (Figure 2d left). Hence, there appears to be an optimal match between the sensor dynamics and the flow velocity that allows extraction of the natural microstructure of chemical plumes.

Chemosensor Array Signal Preprocessing for Chemical Identification. Due to turbulent mixing of eddies governed by the Kolmogorov scale[17] and molecular diffusion governed by the Batchelor scale,[18] chemical filaments become less distinct as we move away from the source, resulting in a less intermittent and more homogeneous chemical signal.[13] This fact was reflected in our results (Figure 3a), as we found both the sensor signal power and intermittency in the signal reduced with increasing distance.

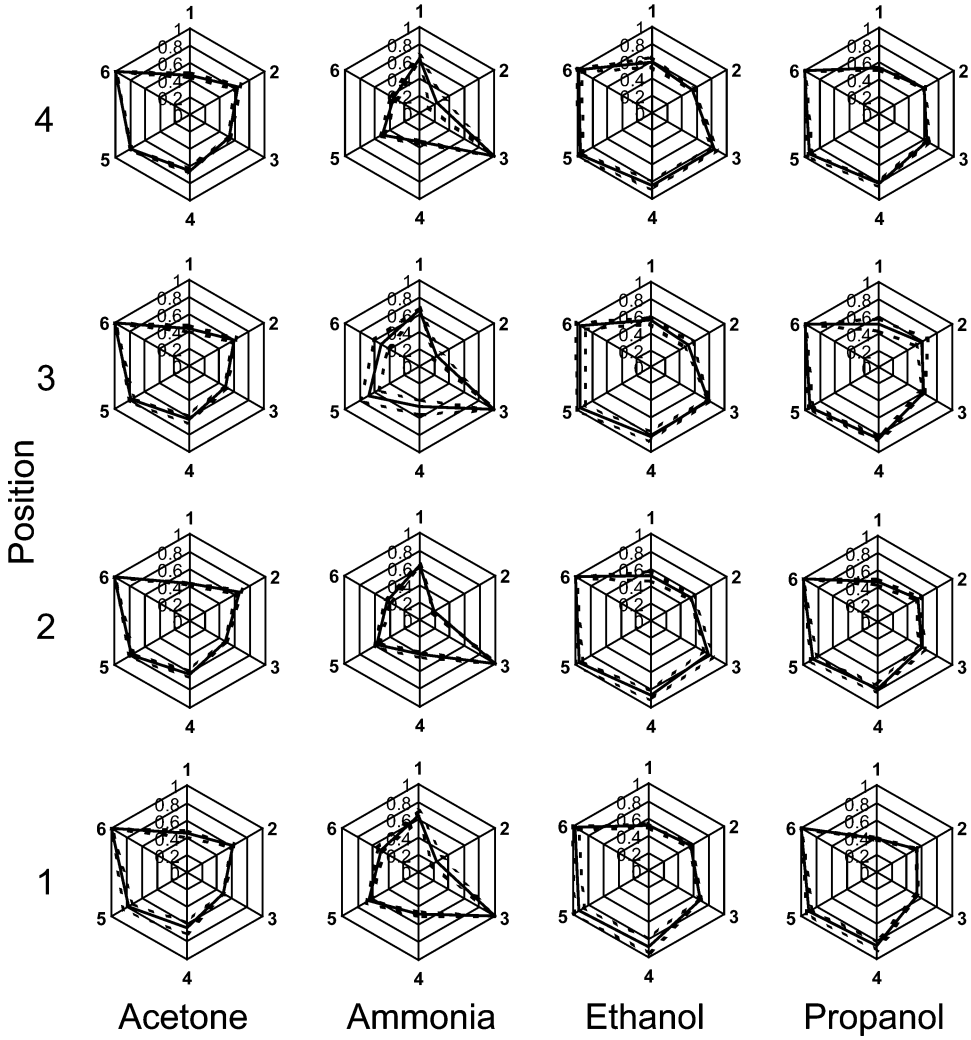

Figure 5. Radar plots showing the 6-element sensor array responses to different chemicals at different positions within the plume, using normalized sensor variation (see methods). Solid lines indicate the means of 4 repeat trails. Dashed lines indicate the ± 1 standard deviation (SD) (flow velocity 0.56 m s^{-1}, position along centerline, (1) 40, (2) 80, (3) 120, and (4) 160 cm).

We were interested in the effect of different source compounds on the instantaneous chemosensor responses as a prelude to solving the chemical identification problem. Figure 3a shows the six chemosensor responses to four source chemicals (acetone, ammonia, ethanol, propanol) at different distances from the source showing the mean and standard deviation of the original sensor variations over repeated trials. At a given position, the relative signal power between the different chemosensor responses is seen to depend upon the chemical source, indicating potential for source classification.

In order to test directly the hypothesis that the chemosensor signal power contains useful information for identifying the chemical source, we proposed a simple time-invariant measure of chemosensor response, which we term sensor variation. For a given chemosensor time series, x_i, this is simply $\sigma(x_i)/\mu(x_i)$, where σ is the standard deviation and μ is the mean. The sensor variation can be shown to be the chemosensor signal power about the mean divided by the mean itself. Thus, the preprocessing metric represents how much signal energy is being generated by chemical interaction with the sensor normalized for its baseline value (since this effects the signal amplitude). This measures the degree of fluctuation in the signals generated for each sensor, which we saw in Figure 3 depends upon the ligand type, and so provides a method of extracting odor class The relative magnitudes of the sensor variation between the different chemosensors within the array (Figure 3b) are found to be largely preserved at different distances from the source for a given chemical compound, as is evident after normalization (Figure 3c).

Data from different source volumes (Figure 4a) also show similar results; while the sensor variations increase with source volume (Figure 4b), the normalized sensor variations are relatively constant (Figure 4c). These results show that at a given distance from the source normalized sensor variations are source volume invariant over at least 1 order of magnitude.

Exploratory Data Analysis. The normalized sensor variations for each chemical at each of the four different positions are shown by radar plots in Figure 5. The profile of response to ammonia is very distinct from the other chemicals whereas the difference in the profiles for acetone, ethanol, and propanol are more subtle. For instance, sensor variations for sensors 4 and 5 are lower for acetone compared to ethanol and propanol, and sensor 3 gives a higher sensor variation to ethanol than to propanol. Furthermore, it can be seen that, after normalization, the response patterns across the array change little at different distances from the

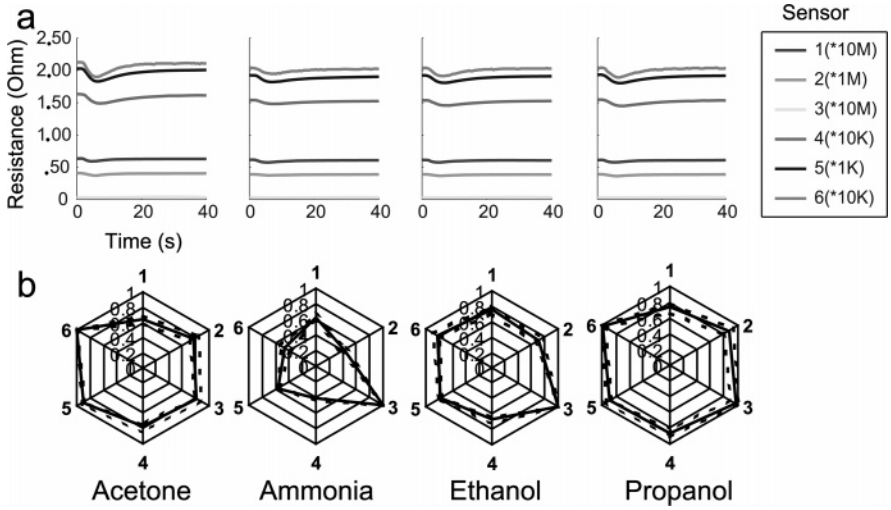

Figure 6. (a) Response of the 6-element chemosensor responding to different chemcial odors under controlled experimental settings. Measurements were taken at 2 Hz. (b) Radar plots showing the 6-element sensor array responses to different chemicals using normalized sensor variation (see methods). Solid lines indicate the means of 10 repeat trails. Dashed lines indicate the ± 1 standard deviation (SD) (sensor baseline values: sensor 1, 6 MΩ; sensor 2, 0.5 MΩ; sensor 3, 1.2 MΩ; sensor 4, 17 kΩ; sensor 5, 2.0 kΩ; sensor 6, 5 kΩ).

Table 1. Details for the DFA Analysis Applied to the Normalized Sensor Variation (Uncontrolled Experimental Environment).

discriminant function	eigenvalue	contribution (%)	cumulative contributio (%)	*p*-value	sensor contributing
Root1	89.54	87.8	87.8	$<10^{-19}$	2,4,5,6
Root2	11.37	11.2	99.0	$<10^{-19}$	2,4,5
Root3	1.06	1.0	100.0	4.07×10^{-10}	3,5,6

source, meaning that the pattern of normalized sensor variances for the same chemical is invariant within the range of distances tested. This indicates that it should be possible to classify an odor independently of its position within some range of distances.

The responses of the same chemosensor array to diluted analytes in a controlled headspace sampler (see Experimental Section) are shown in Figure 6a. The chemosensor responses from the wind tunnel experiments (Figure 3) are far more complex temporally, resulting from the unsteady flow conditions inherent to chemical plumes at these velocities.[14] There was an obvious increase in baseline resistance for the controlled tests that may be related to a cooling effect of the flow in the wind tunnel. Although the baseline resistance values varied considerably between the two conditions, the sensor variation shows array response profiles qualitatively similar to those found in chemical plume environments (Figure 6b).

Classification Study. In order to test whether the normalized sensor variation patterns across the chemosensor array for different chemical plumes are sufficiently different to identify the chemical source, linear discriminant function analysis (DFA)[15,16] was used. For the purposes of chemical identification, the array responses from all four positions for the same chemical were labeled equivalently. Figure 7a shows how the chemosensor array responses rescaled using the first two linear discriminant functions demonstrate clear separation in the classes (see Table 1 for DFA statistics). When using leaving-one-out cross-validation,[15] 98.44% of the data sets can be classified accurately (one propanol is misclassified as ethanol), which gives an accurate estimation of the true classification accuracy to unseen data (compared to chance at 25%). These results demonstrate that, for the analytes studied, the chemical source may be reliably identified independent from distance using the sensor variation metric. By way of comparison, we ran an identical classification procedure on the same data, but now using the instantaneous signal values (rather than the sensor variations) and time-averaged sensor signals (over the full duration), which yielded odor class classification accuracies of 25 (chance) and 53%, respectively. Thus, the sensor variation is a useful time-invariant preprocessing metric for chemical source identification in plumes.

To demonstrate that the pattern of normalized sensor variations is largely independent of source volume, we applied DFA to the data sets recorded at different source volumes. In this case, all source volumes of the same chemical were labeled equivalently, The classification accuracy fell to 93.75% (DFA plots not shown) after leave-one-out (compared to chance at 25%) demonstrated that DFA based on normalized sensor variations can classify chemicals independently the source volume using the sensor variation metric.

For comparison, we conducted an equivalent DFA for classification of data obtained under controlled conditions (Figure 6), the results of which are shown in Figure 7b. The separation in the data are largely equivalent to the chemical classification in plume data but more separation evident between propanol and ethanol, resulting in a classification accuracy of 100% after leave-one-out cross-validation.

Finally, we wanted to understand the time properties of the sensor variation measure we have considered for chemical plume identification. Due to the time-varying nature of the chemosensor

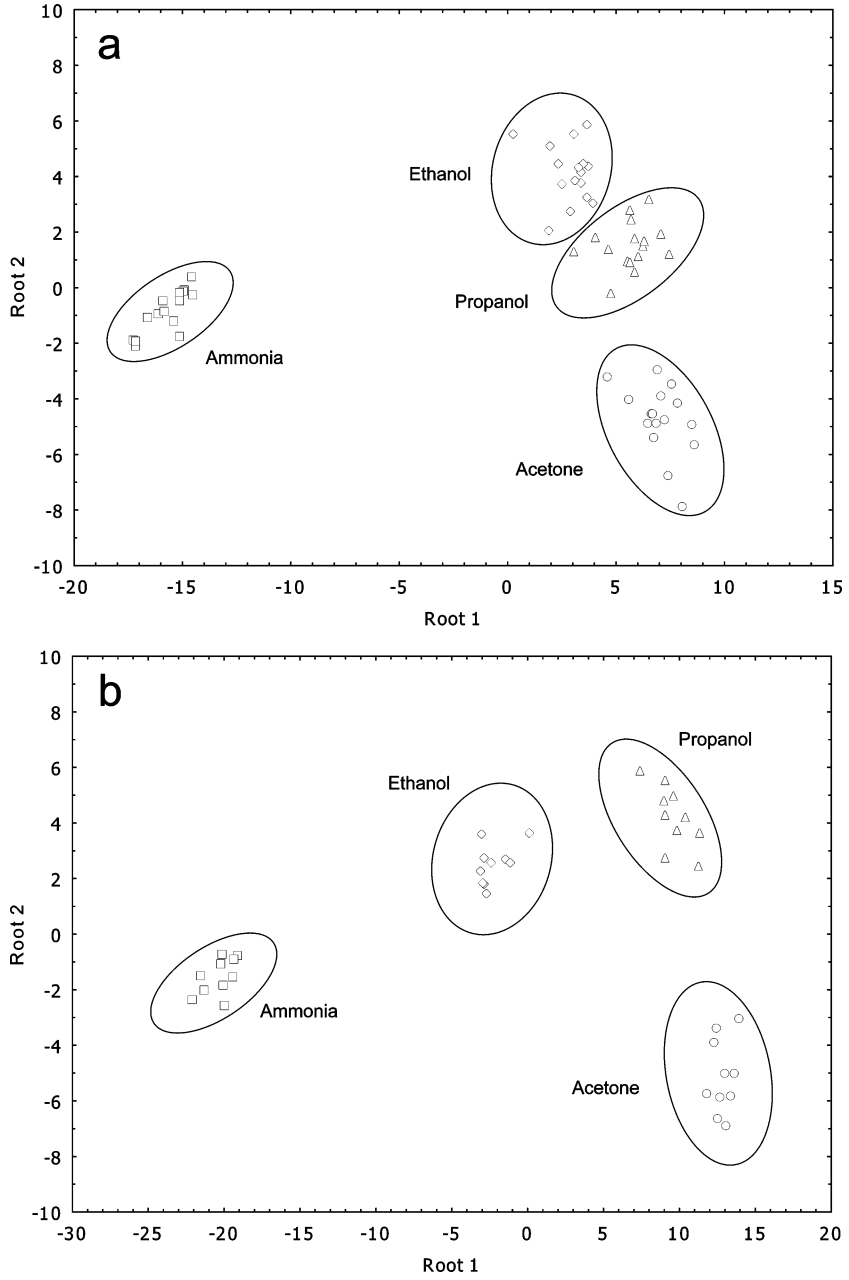

Figure 7. Results of DFA applied to the normalized sensor variation (see methods). (a) Under uncontrolled experimental environment. (b) Under controlled experimental environment.

Table 2. Details for the DFA Analysis Applied to the Normalized Sensor Variation (Controlled Experimental Environment).

discriminant function	eigenvalue	contribution (%)	cumulative contribution (%)	*p*-value	sensor contributing
Root1	187.78	92.0	92.0	$<10^{-19}$	3,5
Root2	14.65	7.2	99.1	$<10^{-19}$	3,4,5
Root3	1.75	1.0	100.0	6.31×10^{-7}	1,4

array signals, the instantaneous chemosensor array response is not a reliable indicator of chemical source. Rather, the signals must be integrated in some way in order to remove the variation due to local concentration changes resulting from turbulent eddies. An important issue is how long must the time-varying time signals be integrated in order to provide a reliable fingerprint of the chemical source. To study this we constructed repeated DFAs using different record lengths from the original data-set to calculate the sensor variation. We did this to calculate the classification accuracy as a function of record length as an indicator of integration time required to achieve reasonable chemical source identification accuracy, the results of which are

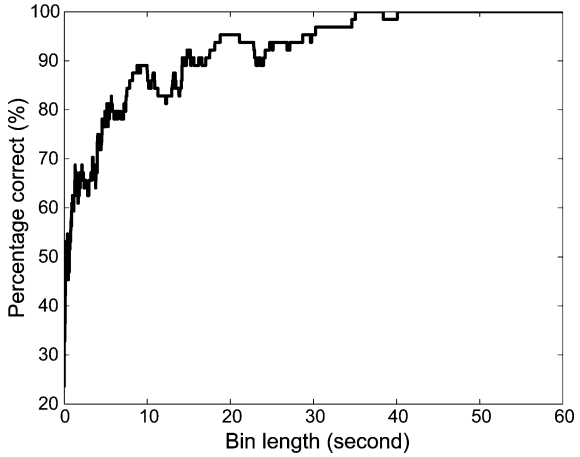

Figure 8. Accuracy of classification under different sampling durations, from 2 ms up to 60 s (leave-one-out method applied).

shown in Figure 8. For this four-class problem, we found that over 90% classification accuracy is achieved after ~20 s and perfect classification of the data set is achieved after 40 s. Thus, some integration time is required to achieve a stable fingerprint of the chemical source, which maybe be further improved by considering the instantaneous or local dynamics of the chemosensor time series.

CONCLUSIONS

Remote chemical source identification is an important problem in a wide variety of domains where the natural fluid dynamics dictate the chemical signal received by any analytical instrument. We have considered the use of chemosensor arrays as a method for source identification in turbulent plumes, which has parallels to olfactory processing in insects operating within such environments. Our results demonstrate that source identification is possible in relatively uncontrolled chemical plume environments with equivalent accuracy to controlled conditions for the compounds, distances and concentrations test in this study.

ACKNOWLEDGMENT

The authors are grateful to the European Commission for funding the research described in this paper under the project "A Fleet of Artificial Chemosensing Moths for Distributed Environmental Monitoring (AMOTH)" funded under the IST Future and Emerging Technologies Program (awarded to T.C.P.). Grant reference IST-2001-33066, project website http://www.amoth.org/).

Received for review May 21, 2007. Accepted August 17, 2007.

AC0710376